

Monte Carlo Simulation for Particles Confined by Thermal Walls

Fangyi Guo, and Carter Matties

October 22, 2025

Abstract

We simulate two-dimensional particle systems using Monte Carlo methods to study the emergence of thermodynamic behavior from microscopic dynamics. Two models were implemented: a harmonic trap and a hard-particle gas confined by thermal walls. Particle motion is integrated using the symplectic Euler method, and thermalization is achieved through probabilistic wall scattering. Random sampling methods, including rejection sampling for Gaussian velocity components and inverse CDF sampling for Maxwell-Boltzmann speeds, are implemented.

We show that observed computational complexity scalings agree with theoretical estimates: $\mathcal{O}(N)$ for the harmonic case and $\mathcal{O}(N^2)$ for hard particle collisions. As results of the simulations, the harmonic system reproduces Gaussian position and velocity distributions and satisfies the equipartition theorem. The hard-particle model yields the expected Maxwell-Boltzmann speed distribution and the ideal gas law. These results validate our methods and demonstrate accurate physical and computational behavior of the models.

Contents

1	Introduction	2
2	Analytic Review	3
2.1	Hard Particle	3
2.2	Harmonic Potential	4
3	Numerical Methods	5
3.1	Rejection Sampling and Inverse CDF	5
3.2	Validation	6
3.3	Computational Complexity	7
4	Results and Discussion	9
4.1	Maxwell-Boltzmann Distribution	9
4.2	Pressure	10
4.3	Equipartition	11
5	Conclusion	12

1 Introduction

Monte Carlo (MC) methods play an important role in modern computational physics, allowing complex statistical systems to be sampled and analyzed through stochastic simulation without analytical integration. In this project, we use a series of particle simulations that implement Monte Carlo methods to investigate the emergence of thermodynamic properties in simple classical systems, including Maxwell-Boltzmann distribution, the equipartition theorem, and the ideal-gas law. Although the equation of motion can be integrated deterministically, the statistical ensemble is generated stochastically through randomized initial conditions and probabilistic wall interactions. These processes require repeated sampling over long time evolutions, leading to Monte Carlo methods.

Our study is organized as two complementary models. The first studies a hard-particle gas in a square box with thermal walls. The particles move freely and collisions between them occur. Monte Carlo randomness enters through diffuse wall reflections that re-thermalize particles at the wall temperature T_{bath} . For a long enough time, the speed distributions of the particles follow a 2D Maxwell-Boltzmann distribution at temperature T_{bath} theoretically, which is expected to be reproduced by the simulation. For these non-interacting particles, we also track the relationship between pressure and temperature, which verifies the two-dimensional ideal-gas law $pA = Nk_{\text{B}}T$.

The second part of the project studies particles in a box with thermal walls, but are also confined in a two-dimensional harmonic trap. By sampling particle positions and velocities over time, we construct histograms that can be directly compared to theoretical Gaussian distributions predicted by the Maxwell-Boltzmann statistics. The harmonic potential has the property that the Hamiltonian contains only quadratic degrees of freedom, which satisfy the equipartition theorem

that each quadratic degree of freedom contributes an average energy of $\frac{1}{2}k_{\text{B}}T$. These results verifies that random sampling and ensemble averaging recover the expected equilibrium behavior.

This project aims to demonstrates how random processes under Monte Carlo methods can be integrated into simple particle models to reproduce results in thermodynamics and statistical mechanics. By connecting microscopic dynamics with macroscopic observables through controlled stochasticity, the simulations provide a clear illustration of how statistical results emerge from random particle motions.

2 Analytic Review

For the purpose of comparing and validating the numerical methods, we briefly go over the analytic solutions in this section. Rather than giving a complete derivation, we list key results of the models, which will be verified by numerical methods in the next sections

Consider a 2D system containing a large number of identical non-relativistic particles confined by thermal walls with temperature T . The particles move according to the equation of motion

$$m\ddot{r}_i = -\nabla V(r_i), \quad (2.1)$$

where i denotes the i 's particle, and V is some potential. In this project, we will focus on two specific potentials, the trivial one and the harmonic potential.

2.1 Hard Particle

For the trivial case, the particles move freely in the box. We will focus on the interaction of the particles and the walls, and model it in the following way. When a particle hits the wall, there is a probability p that it will have an elastic collision, leading to the specular reflection

$$v_{\perp} \rightarrow -v_{\perp}, \quad v_{\parallel} \rightarrow v_{\parallel} \quad (2.2)$$

i.e., changing the sign for the perpendicular component and leaving the parallel component unchanged. The particle also has the probability $1 - p$ to have a thermal reflection in which the wall acts as a thermal bath at temperature T . The particle picks up a new velocity sampled from a Maxwell-Boltzmann distribution of thermal velocities at that temperature

$$f(v_x, v_y) = \frac{m|\mathbf{v}|}{k_{\text{B}}T} \exp\left(-\frac{m|\mathbf{v}|^2}{2k_{\text{B}}T}\right), \quad (2.3)$$

where $|\mathbf{v}| = \sqrt{v_x^2 + v_y^2}$ is the velocity norm, m is the mass of the particle, k_{B} is the Boltzmann constant. This is a natural result of velocity for particles acquiring a temperature T by contacting the thermal wall. This stochastic resampling is the Monte Carlo step, randomizing the velocity vector according to physical probability distributions.

All particles start with arbitrary positions and velocities, and evolve according to the equation of motion (2.1). For each time step, the position is determined by

$$r_i(t + \Delta t) = r_i(t) + \mathbf{v}_i(t)\Delta t. \quad (2.4)$$

Since particles do not have interactions in this case, the iterative steps are simple. After a long enough time, the velocity distribution is driven to equilibrium and expected to obey the Maxwell-Boltzmann distribution

$$P(v) dv = \frac{mv}{k_B T} \exp\left(-\frac{mv^2}{2k_B T}\right) dv. \quad (2.5)$$

Here, v represents the magnitude of the velocity and $P(v)$ denotes the probability of the velocity between v and $v + dv$. In fact, at equilibrium all particles have the same temperature T with the wall, and they should exhibit the same Maxwell-Boltzmann distribution.

To validate the model and methods, we will check several physical quantities of the system and compare with their analytic anticipations.

In thermodynamics, the pressure of particles in a box is the result of collisions between the particles and the wall. Concretely, pressure is defined by the momentum transfer of particles per unit time per unit area. In fact, if collisions occur i times, then the pressure is given by

$$p = \frac{1}{A\Delta t} \sum_i 2m|v_{\perp,i}|, \quad (2.6)$$

where A is the area of the wall, Δt is the time step, and $v_{\perp,i}$ is the normal velocity to the wall. At equilibrium of the simulation, the pressure of the system is expected to satisfy the ideal gas law

$$pA = Nk_B T, \quad (2.7)$$

where N is the number of particles. Hence, we expect the simulation result of pressure to be linearly related to temperature.

Another physical quantity that can be checked in the simulation is the mean kinetic energy. For the thermal system, the mean kinetic energy per particle is theoretically given by

$$\frac{1}{2}m\langle v^2 \rangle = k_B T. \quad (2.8)$$

2.2 Harmonic Potential

An extension of the model is to add a nontrivial potential $V(r)$ to the system. In this project, we will focus on the harmonic potential

$$V = \frac{1}{2}k(x^2 + y^2), \quad (2.9)$$

and resulting physical properties. The equation of motion (2.1) becomes

$$m\ddot{\mathbf{r}}_i = -\mathbf{k} \cdot \mathbf{r}, \quad (2.10)$$

where $\mathbf{k} = (k_x, k_y)$ is the spring constant with k_x, k_y corresponding to two directions. The process can be simulated via the ODE methods used in the last project, such as the symplectic method and the Runge-Kutta method. In this project, we will use the symplectic Euler method to solve the ODE. For nontrivial potentials, the speed distribution is also expected to be Maxwell-Boltzmann. However, for a canonical ensemble at temperature T with Hamiltonian H , the probability density

over phase space is

$$f(x, p) \propto \exp(-\beta H(x, p)), \quad (2.11)$$

where $\beta = 1/k_B T$. For a harmonic trap, this becomes

$$f(x, p) \propto \exp\left[-\beta\left(\frac{1}{2}m(v_x^2 + v_y^2) + \frac{1}{2}k_x x^2 + \frac{1}{2}k_y y^2\right)\right]. \quad (2.12)$$

Note that although the speed magnitude has a Maxwell-Boltzmann distribution, each position component and each velocity component have a Gaussian distribution. Specifically, each x and y are Gaussian with variance $\sigma_x^2 = k_B T/k_x$ and $\sigma_y^2 = k_B T/k_y$; each v_x and v_y are Gaussian with variance $\sigma_{v_x}^2 = \sigma_{v_y}^2 = k_B T/m$. This provides a way to validate our methods. In a long enough time, the simulation should reproduce these Gaussian distributions if we track each degree of freedom.

Note that for the harmonic potential, the Hamiltonian of the particle has quadratic degrees of freedom. As a result, the average kinetic and potential energy satisfy the equipartition theorem,

$$\left\langle \frac{1}{2}mv_x^2 \right\rangle = \left\langle \frac{1}{2}mv_y^2 \right\rangle = \left\langle \frac{1}{2}kx^2 \right\rangle = \left\langle \frac{1}{2}ky^2 \right\rangle = \frac{1}{2}k_B T. \quad (2.13)$$

In other words, if we denote the kinetic energy and the potential energy as K and V , they are expected to be

$$\langle K \rangle = \langle V \rangle = k_B T. \quad (2.14)$$

This analytical statement will also be tested using the simulation result.

3 Numerical Methods

In this section, we will briefly introduce the numerical methods for the simulation and study their properties. We start by introducing two important sampling methods that are used in the probabilistic interactions, and then analyze the computational complexity for the simulation. Finally, we show results from the simulation and justify our methods by comparing with expected behaviors.

3.1 Rejection Sampling and Inverse CDF

In order to generate random particle velocities consistent with the desired thermal equilibrium, two probabilistic sampling techniques are employed - rejection sampling and the inverse cumulative distribution function (CDF) method. These methods allow one to numerically draw samples from target probability distributions when direct sampling is inconvenient.

For the thermal initialization of particle velocities in the harmonic and gas-box systems, we require components of the velocity to have Gaussian distribution

$$v_x, v_y \sim \mathcal{N}(0, \sigma^2), \quad (3.1)$$

where

$$\sigma^2 = \frac{k_B T}{m}. \quad (3.2)$$

The probability density function (PDF) of each velocity component is

$$p(v) = \frac{1}{\sqrt{2\pi}\sigma^2} \exp\left(-\frac{v^2}{2\sigma^2}\right). \quad (3.3)$$

Note that this PDF is maximized at $v = 0$ with function value $p(0) = (2\pi\sigma^2)^{-1/2}$. To implement rejection sampling, we pick a rectangular region $[-5\sigma, 5\sigma] \times [0, p(0)]$ which encloses the PDF, and draw a candidate (v', y) uniformly in that region. v' is accepted if y falls below the PDF, i.e. $y < p(v')$; otherwise this candidate is rejected and we resample. This procedure produces values distributed according to the desired normal law. We use rejection sampling here rather than the inverse CDF method because it does not require an explicit analytic form for the cumulative distribution function (CDF), which in fact does not exist for Gaussian distributions.

When the particle hits the thermal wall, it picks up a velocity according to the Maxwell-Boltzmann distribution, which describes the velocity distributions of particles at thermal equilibrium at temperature T . In two dimensions, the Maxwell-Boltzmann distribution is

$$f(v) = \frac{mv}{k_B T} \exp\left(-\frac{mv^2}{2k_B T}\right), \quad v \geq 0. \quad (3.4)$$

Its cumulative distribution function (CDF) can be integrated analytically as

$$F(v) = \int_0^v f(v') dv' = 1 - \exp\left(-\frac{mv^2}{2k_B T}\right). \quad (3.5)$$

To sample from $f(v)$ using the inverse CDF method, we invert the CDF

$$v = F^{-1}(u) = \sqrt{-\frac{2k_B T}{m} \log(1 - u)}, \quad (3.6)$$

and picks u uniformly from 0 to 1. Compared to the rejection sampling method, this provides an efficient way to generate speeds that satisfy Maxwell-Boltzmann distribution.

Note that this sampling from the Maxwell-Boltzmann distribution only gives the speed magnitude. After collisions with the wall, particles also pick a direction of their velocities. To complete the sampling procedure, we pick the azimuthal angle θ uniformly between 0 and 2π , leading to the components

$$v_x = v \cos \theta, \quad v_y = v \sin \theta. \quad (3.7)$$

This concludes the sampling methods we implement in the simulation and ensures that the initial and boundary thermalization steps accurately reproduce the equilibrium temperature T .

3.2 Validation

To ensure that our numerical scheme and random sampling methods correctly reproduce equilibrium statistical mechanics, we validated the implementation using the harmonic trap system, where the analytic equilibrium distributions are known exactly.

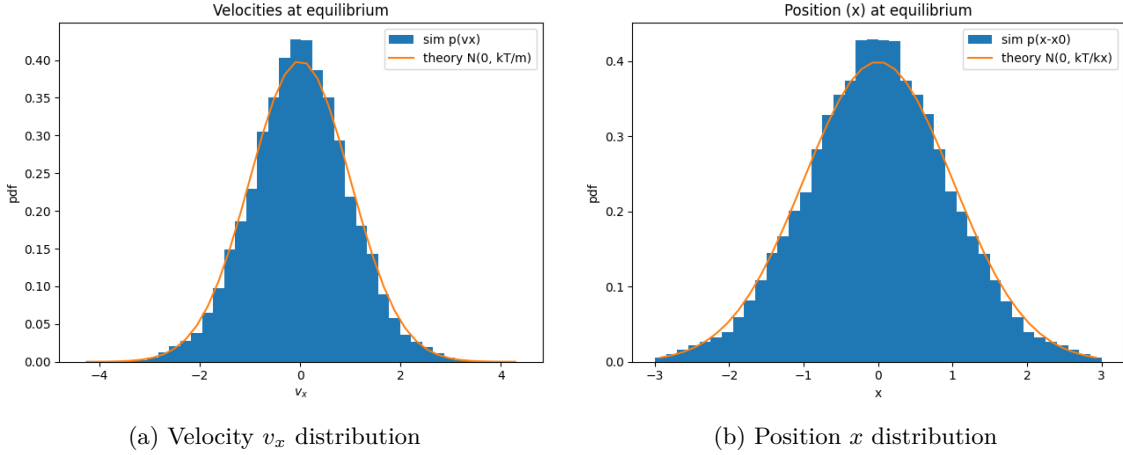


Figure 1: Distribution of velocity v_x (left) and position x (right) at steps 50000 with step 0.001. The analytic distribution in orange curve is Gaussian for both velocity and position. The histogram of simulation results shows agreement with the Gaussian distributions.

As is shown in Section 2.2, for a particle of mass m in a two-dimensional harmonic potential

$$V(x, y) = \frac{1}{2}k_x(x - x_0)^2 + \frac{1}{2}k_y(y - y_0)^2, \quad (3.8)$$

the canonical distribution at temperature T predicts that both the position and velocity components follow Gaussian laws:

$$p(x) = \sqrt{\frac{k_x}{2\pi k_B T}} \exp\left[-\frac{k_x(x - x_0)^2}{2k_B T}\right], \quad p(v_x) = \sqrt{\frac{m}{2\pi k_B T}} \exp\left[-\frac{mv_x^2}{2k_B T}\right]. \quad (3.9)$$

We performed long-time integrations using the symplectic Euler method, with velocities and positions sampled periodically after equilibration. Figure 1 shows the resulting histograms of v_x and $x - x_0$ with their respective analytic Gaussian distributions. The excellent agreement between simulation and theory confirms that the system correctly samples the canonical ensemble.

From the two examples, we validate our methods of motion integration and probabilistic interactions. It demonstrates that the combined use of rejection sampling (for Gaussian velocity components) and inverse CDF sampling (for Maxwell–Boltzmann magnitudes) yields statistically consistent equilibrium states. Consequently, all subsequent measurements, such as equipartition relations, pressure–temperature dependence, and computational scaling, can be interpreted as physically meaningful within the framework of classical statistical mechanics.

3.3 Computational Complexity

For N particles, the overall time complexity to run our simulation for T time steps with hard particles is

$$\mathcal{O}(N^2 T),$$

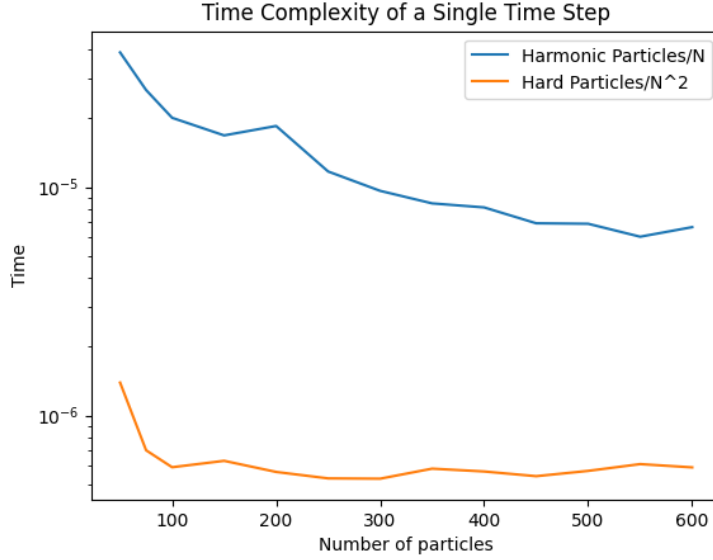


Figure 2: Time complexity scaling of the function which evolves the simulation by 1 time step. Note that the time to evolve hard particles, divided by N^2 , quickly approaches a constant value. Additionally, the time to evolve particles in a harmonic potential, divided by N , is approaching a constant value, albeit more slowly.

and the time complexity to run our simulation with non-interacting particles in a harmonic potential is

$$\mathcal{O}(NT).$$

The steps to evolve our simulation by a single time step are as follows:

1. Evolve each particle's position and velocity by 1 time step using the symplectic form of Euler's method,
2. Compute particle-particle interactions,
3. Compute particle-wall interactions.

The first step has a time complexity of $\mathcal{O}(1)$ per particle, as we have seen before, so the overall time complexity of this step is $\mathcal{O}(N)$.

The third step also has time complexity $\mathcal{O}(N)$. Although this computation requires us to compare a particle's position to the wall positions, generate a random number to determine if a specular or diffuse reflection occurs, and then generate a random number to determine the new velocity if the reflection is diffuse, all for each particle, all of these operations are $\mathcal{O}(1)$ per particle. In particular, no operations which we perform for each particle have greater time complexity than $\mathcal{O}(1)$. Thus, this step contributes complexity $\mathcal{O}(N)$ per time step.

Finally, the second step, computing particle-particle interactions, has time complexity $\mathcal{O}(N^2)$ because we need to compute the interaction for each pair of particles. In particular, we generate a pair of $N \times N$ matrices representing the relative distances and the relative velocities between each pair of particles; generating each of these matrices must be an $\mathcal{O}(N^2)$ operation. In particular, although we generate these $N \times N$ matrices, every operation on them is performed element-wise; thus, the maximum time complexity for any operation in this step is $\mathcal{O}(N^2)$.

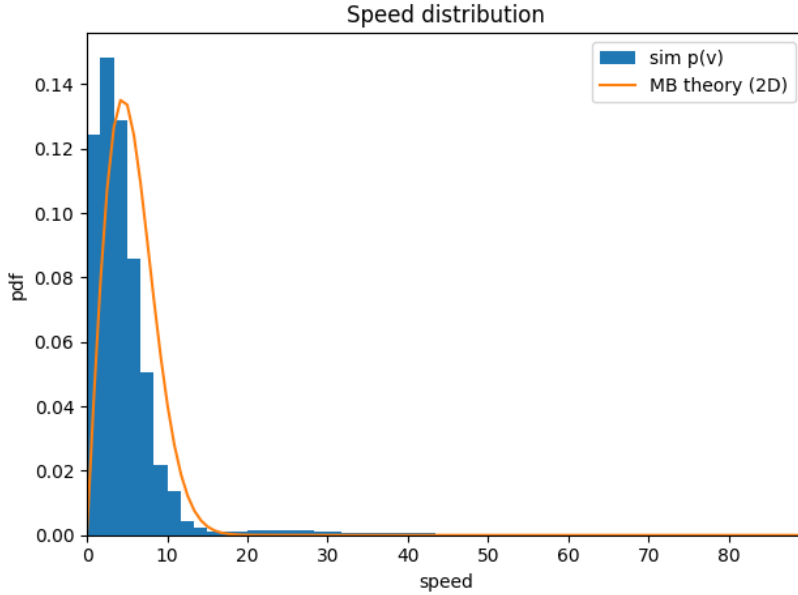


Figure 3: Average observed particle speed distribution after 25,000 time steps of burn in, compared with the theoretical prediction of the Maxwell-Boltzmann distribution (Eqn. 2.3). The observed distribution has approximately the same shape as the theoretical prediction, but skewed toward smaller speeds.

Note that, in both the harmonic and the hard particle cases, we evolve the particles with Euler’s method and compute particle-wall interactions, we do not compute particle-particle interactions in the harmonic case. Additionally, we perform each the three steps exactly once for each time step. Therefore, in the harmonic case, we have a time complexity of $\mathcal{O}(N)$ per time step, or $\mathcal{O}(NT)$ overall, and in the hard particle case, we have a time complexity of $\mathcal{O}(N^2)$ per time step, or $\mathcal{O}(N^2T)$ overall.

Indeed, plotting the time to evolve our simulation by a single time step for both harmonic and hard particles, we find that the observation is in good agreement with our theoretical time complexities of $\mathcal{O}(N)$ and $\mathcal{O}(N^2)$, respectively (Fig. (2)).

From Fig. (2), we see that the time complexity to evolve hard particles by one time step does, indeed, quickly approach N^2 . However, the time complexity to evolve harmonic particles by a single time step approaches $\mathcal{O}(N)$ more slowly. This is likely because there are some $\mathcal{O}(1)$ overhead operations which quickly become negligible with $\mathcal{O}(N^2)$ scaling, but continue to matter for larger N when the time complexity scales as $\mathcal{O}(N)$, as is the case for harmonic particles.

4 Results and Discussion

4.1 Maxwell-Boltzmann Distribution

An important relation governing the long-term behavior of the speeds of a collection of thermal particles is the Maxwell-Boltzmann distribution (Eqn. (2.3)). Here, we investigate this distribution using an ensemble of particles with elastic collisions but no other particle-particle interactions, in a box with some ambient bath temperature.

We run our simulation of hard particles with a box size of 1, an ambient bath temperature of

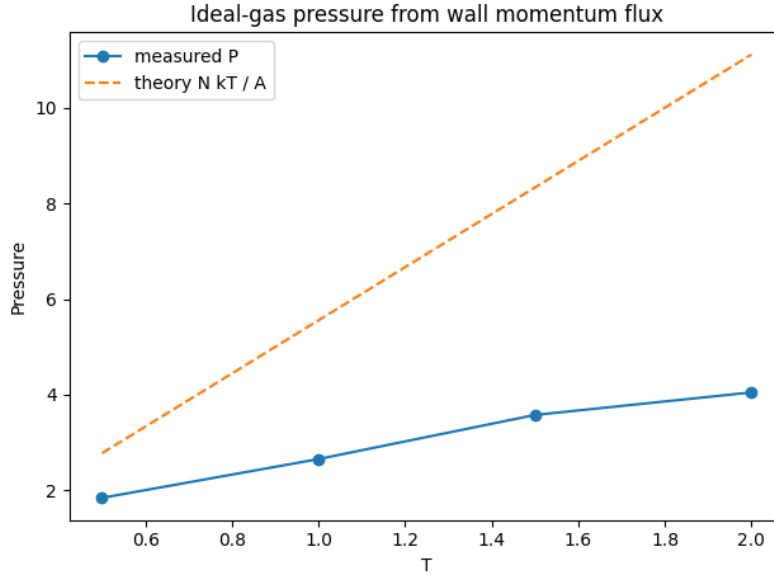


Figure 4: Average pressure exerted on the container by a gas of hard particles as a function of ambient bath temperature. Although our measured relationship does not match the theoretical prediction, it is still linear.

1, a particle radius of 0.02 and a probability of specular reflections of 0.2.

Initially distributing particles uniformly across the box and giving them initial velocities whose x and y components are each selected from a Gaussian distribution. We then let the simulation “burn in” for 25,000 time steps without sampling the speed. Finally, we run the simulation for another 50,000 time steps, when we sample the speed distribution every 80 time steps.

Under this setup, we observe the average speed distribution given in Fig. (3). From this plot, we can see that our observed distribution has a similar shape to that of the precise theoretical Maxwell-Boltzmann distribution, but our observations are skewed toward a lower mean speed than the theory dictates.

Although our observed speed distribution differs from the theory, it appears similar to a Maxwell-Boltzmann distribution at some smaller temperature. This provides some evidence for the fact that, although we allow the simulation to run for a large number of time steps (25,000 before we begin measuring), our choice of $dt = 0.001$ might be too small and not enough total time is passing for the particles to reach thermal equilibrium with the bath.

4.2 Pressure

We run our simulation of hard particles again for various ambient bath temperatures. In particular, we run our simulation in a box of size 6, particles of radius 0.02, and a specular reflection probability of 0.4. We then run this simulation of $N = 200$ particles for four different values for the ambient bath temperature, and record the total momentum transferred between particles and the wall for each sampled time step. Then, we compute the pressure at each time step from these momenta using Eqn. (2.6), and plot the average pressure as a function of bath temperature in Fig. (4).

From this plot, we can see that we have an approximately linear relationship between pressure and temperature, in agreement with the theoretical prediction of the ideal gas law. However, our measurements appear to differ from the theory by some constant factor ≈ 2 . This discrepancy is

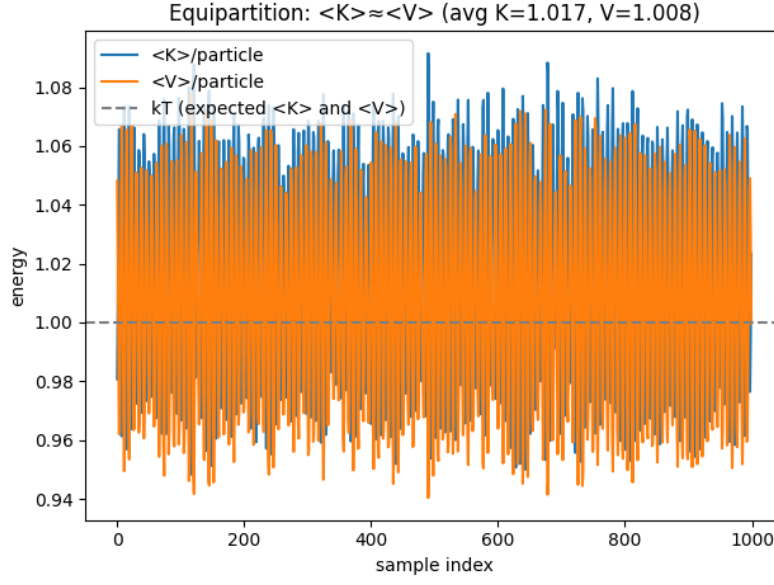


Figure 5: Time evolution of average kinetic ($\langle K \rangle$) and potential ($\langle V \rangle$) energy per particle for the harmonic trap at $T = 1.0$. Both fluctuate around $k_B T$ (dashed line), confirming the equipartition theorem. The measured averages $\langle K \rangle = 1.017k_B T$ and $\langle V \rangle = 1.008k_B T$ yields relative deviations below 2%.

most likely due to some error in our computation of the total momentum transferred, or somewhere else in our implementation of Eqn. (2.6).

In particular, the discrepancy between theory and our observations is likely not due to numerical integration error, nor is it due to finite precision. This discrepancy is most likely not due to finite precision error because the ratio between the measured and theoretical pressure is (approximately) constant. Since we are simply summing along the changes in momentum, we would expect any accumulated finite precision error to be constant, rather than proportional to the measured pressure.

4.3 Equipartition

Another important relation to test is the equipartition theorem. As is introduced in Section 2.2, we run the harmonic trap system with a time step 0.01 for a total of 40,000 integration steps. The system was initialized with velocities and positions sampled from a Gaussian distribution using rejection sampling method, and energy values were recorded periodically after an initial transient period. The time series of the mean kinetic energy per particle, $\langle K \rangle$, and the mean potential energy per particle, $\langle V \rangle$, are shown in Fig. 5. Both quantities fluctuate around the theoretical prediction of $k_B T$ with no systematic drift observed.

Quantitatively, we obtain $\langle K \rangle = 1.017k_B T$ and $\langle V \rangle = 1.008k_B T$, corresponding to relative deviations of about 1.7% and 0.8% from the theoretical expectation. These discrepancies are well within the range of noise expected from stochastic thermal fluctuations.

The result verifies the equipartition theorem expected for our system at thermal equilibrium. The agreement provides another strong evidence that the system has reached thermal equilibrium and reproduces statistical quantities. This test also confirms the validity of the velocity sampling procedures, including rejection sampling from a Gaussian distribution and inverse CDF sampling from a Maxwell-Boltzmann distribution.

5 Conclusion

In this project, we implemented simulations with Monte Carlo methods to study the emergence of thermal equilibrium and macroscopic thermodynamic laws from microscopic particle dynamics. By combining deterministic time integration with probabilistic wall interactions, the model successfully bridges classical mechanics and statistical physics.

In the harmonic potential system, we studied particles under a quadratic potential. Modeling as probabilistic interactions and sampling from reasonable distributions, we validated our method by plotting positions and velocities and verified the equipartition theorem at equilibrium. For the hard particle model, we reproduced the Maxwell-Boltzmann distribution and tested the ideal gas law. The simulation results are shown to be consistent with the expected result with small errors.

From a computational perspective, we use rejection sampling and inverse CDF sampling in the simulation to ensure statistically correct initialization and thermalization. We also studied time complexity of a single step in terms of the number of particles, and showed that our observation is in good agreement with the theoretical time complexities.

The simulations with Monte Carlo approach not only visualize how random processes give rise to predictable macroscopic observables, but also offer a practical framework for bridging probability theory, numerical methods, and various branches in physics.